Research Article

Advances in Mechanical Engineering

Advances in Mechanical Engineering
2016, Vol. 8(5) 1–10

DOI: 10.1177/1687814016649354
aime.sagepub.com
SAGE

Microstructural morphology of rheocast A319 aluminium alloy

Ahmad Muhammad Aziz[1], Mohd Zaidi Omar[1,2], Zainuddin Sajuri[1,2] and Mohd Shukor Salleh[3]

Abstract

This article examines the evolution of the microstructure of A319 aluminium alloy as it flows along a cooling slope plate and discusses the type and influence of the intermetallic compounds thus formed. Numerous past research studies have analysed the microstructural transformation of alloys in a mould, but few researchers have investigated this phenomenon on the cooling slope plate. A change in the microstructure of the alloy from dendritic to non-dendritic is clearly obtained as the alloy moves from the impact zone to bottom zone on the cooling slope plate. It is important to clarify the mechanism of microstructural evolution through nucleation and fragmentation of the primary phase arm for fundamental understanding of research. Analysis by optical microscope and scanning electron microscope reveals the evolution of the microstructure and intermetallic compounds of A319 as it progresses along the cooling slope plate. The Vickers test was used to determine the hardness of the alloy thus produced. The results show the influence of the mould in obtaining a spheroidal microstructure; the microstructure in the bottom zone of the cooling slope plate is nearly spheroidal rather than fully spheroidal. The hardness of the alloy is enhanced when the microstructure is spheroidal and when the Mg_2Si compound is present in the alloy.

Keywords

Semi-solid processing, cooling slope, nucleation, evolution, intermetallic compound

Date received: 28 October 2015; accepted: 20 April 2016

Academic Editor: Liyuan Sheng

Introduction

Over the past 40 years, semi-solid metal (SSM) processing has been explored by numerous researchers interested in exploiting the attributes of the unique properties of metallic microstructures. After SSM processing, the microstructure of a metallic alloy becomes spheroidal rather than dendritic. This spheroidal microstructure is important as it enables easy movement in the primary phase of α-Al when an external load is exerted on a material compared to a dendritic microstructure that is characterized by interlocking between the grains, which makes the material resistant to movement.[1]

Several techniques have been developed to transform microstructures. These can be grouped into three categories: (1) the liquid method route, which includes magneto hydrodynamic (MHD) stirring, cooling slope (CS) casting and spray deposition; (2) the solid-state

[1]Department of Mechanical and Materials Engineering, Faculty of Engineering and Built Environment, Universiti Kebangsaan Malaysia, Bangi, Malaysia
[2]Centre for Automotive Research, Faculty of Engineering and Built Environment, Universiti Kebangsaan Malaysia, Bangi, Malaysia
[3]Department of Manufacturing Process, Faculty of Manufacturing Engineering, Universiti Teknikal Malaysia Melaka, Durian Tunggal, Malaysia

Corresponding author:
Mohd Zaidi Omar, Department of Mechanical and Materials Engineering, Faculty of Engineering and Built Environment, Universiti Kebangsaan Malaysia, 43600 Bangi, Selangor, Malaysia.
Email: zaidiomar@ukm.edu.my

Table 1. Chemical composition of aluminium alloy A319.

Si	Cu	Fe	Mg	Zn	Mn	Cr	Al
6.15	2.12	0.72	0.44	0.4	0.13	0.05	Remaining

route, which includes processes such as strain-induced melt activation (SIMA) and recrystallization and partial melting; and (3) combination methods such as the self-inoculation method and CS with vibration.[2] The CS casting process is the simplest in terms of equipment and handling and is able to produce globular microstructures from the dendritic microstructure.[3–5] The CS casting process is 'lab friendly' because fewer items of equipment are required:[6] a furnace to melt the alloy, a CS plate for the molten alloy to flow down and a mould to collect the molten alloy where it solidifies.

In SSM processing, two main routes have been developed to produce a globular microstructure in alloys: thixoforming and rheocasting. The thixoforming process has two additional steps compared to rheocasting: solidifying the billet and preheating prior to forming the billet.[7]

Aluminium alloys are widely used in automotive manufacturing, especially aluminium–silicon (Al-Si) alloys due to their low density, high strength/weight ratio and excellent castability.[8] These alloys are particularly suitable for use in components such as cylinder heads, pistons and cylinder blocks.[9] The microstructure of Al-Si alloys consists of a mixture of a primary phase and a eutectic phase of various elements such as eutectic silicon and other intermetallic compounds. Depending on the weight percentage of the base material, Al-Si alloys contain varying amounts of elements such as zinc, copper, magnesium and iron. The size, shape and distribution of the Al-Si second phase has a significant effect on the mechanical properties of the alloys.[10–12] Ideally, the globular microstructure of the primary phase α-Al is surrounded by a layer of eutectic mixture. The eutectic mixture layer acts as a bond between the components of the primary phase and enables the primary phase to resist an exerted external force.

This work focuses on the morphology of aluminium alloy A319 as it progresses down the CS plate during the CS casting process. To the best of the authors' knowledge, only a few research studies[13,14] have been conducted on the rheology of aluminium alloy along the CS plate. Yet, identifying whether the globular microstructure is formed either on the CS plate or in the mould is important for setting parameters that can optimize the time and cost of experiments. The results of this study on the evolution of the microstructure of A319 show that the influence of the mould at the end of the CS is significant because the microstructure obtained in the bottom zone of the CS is a nearly globular microstructure whereas that obtained in the mould is fully globular microstructure. In this study, the mechanism of nucleation and fragmentation in the primary phase in obtaining a near spheroidal microstructure, as well as the formation of intermetallic compounds was also investigated. Moreover, the study determines the hardness of the materials in each zone to verify the evolution of the microstructure.

Table 2. Cooling slope casting parameters.

Angle (°)	Pouring temperature (°C)	Length (mm)
60	630	400

Experiment

The microstructure of aluminium alloy A319 was investigated in this work. The chemical composition of A319 is given in Table 1. The alloy was examined using the X-ray fluorescence (XRF) technique. In XRF, the individual atoms of a sample become energetic when X-ray photons (from an external source) of a characteristic energy or wavelength are directed at the sample. The various elements of the sample such as Si, Mg, Cu and Zn are identified by counting the number of photons emitted by the sample.

Differential scanning calorimetry (DSC) was employed to check the alloy's liquid fraction profile. The semi-solid temperature of A319 can be estimated using the liquid fraction profile in a range between 20% and 50%.[15,16] The pouring temperature and liquidus and solidus temperatures can also be estimated using the liquid fraction profile. The sample was cut into small pieces of approximately 42.7 mg each. The pieces were then melted in a helium environment at 10°C/min to prevent oxidation when using the DSC machine to obtain a liquid fraction profile through the analysis of the partial integral under the endothermic curve.

Three parameters were considered in the CS casting process: the pouring temperature and the length and the angle of the CS. The values of these three parameters were based on the results of the optimization study conducted by Salleh et al.[6] The parameters used in this study are shown in Table 2.

The process of pouring the sample onto the CS began by melting the as-received A319 in an induction

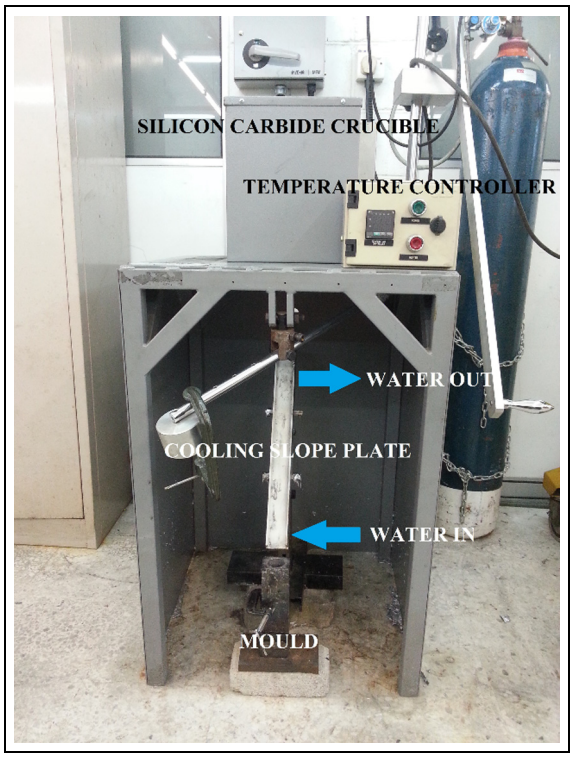

Figure 1. CS apparatus.

heating furnace with a capacity of 2 kg. For this experiment, 400 g of A319 was superheated to 800°C and then allowed to cool to the selected pouring temperature before being poured into 90-mm-wide CS plate made of stainless steel. A K-type thermocouple was placed inside the crucible to ensure that the temperature reading for the molten alloy was equivalent to that shown by the temperature controller. Water was circulated at room temperature underneath the CS plate during the experiment to increase the nucleation rate of α-Al. A thin layer of boron nitride was sprayed onto the CS plate in order to prevent the molten alloy from sticking to the plate and to improve the flow. The molten A319 was poured through a 10-mm-diameter hole of a silicon carbide crucible at 300-mm height above the CS plate, as shown in Figure 1. Rapid quenching occurred on the CS plate upon the poured alloy coming into contact with the plate, and the alloy continued to solidify as it flowed down to the end of the plate, at which point the sample was removed from the CS plate for analysis.

For the analysis, the solidified sample was divided into four zones, namely, impact, top, middle and bottom, as shown in Figure 2. All four zones were cut into pieces using a hand saw in order to analyse the microstructural evolution in each zone. The thickness of the solidified samples was 7 mm, as this thickness is necessary in hot mounting and for convenience in alloy handling, especially during grinding, polishing and microstructural analysis.

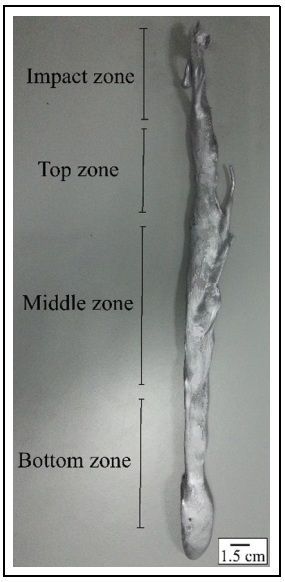

Figure 2. Poured sample of CS casting.

The samples were ground and polished before etching with Keller's reagent for 7 s prior to microstructural image capture with an optical microscope at a magnification of 100 μm. The various phases of the poured samples were identified using a scanning electron microscope (SEM; Zeiss EVOMA 10) equipped with energy-dispersive X-ray (EDX; APOLLO X). The hardness of the material was determined using the Metallic Vickers machine (MITAKA HVS-10), imposing a load of 19.61 N (2 kg) for 10 s. In total, 10 readings were taken for the Vickers measurements, each one in a different position, to obtain an average reading.

Results and discussion

Mechanism of near-spherical formation on the CS plate

The formation of a near-spheroidal microstructure obtained using the CS casting process has been proven by researchers by studying the solidified alloy in the mould.[17] The aim of this research is to study the evolution of this nearly spheroidal formation of the microstructure from the impact zone to the bottom zone of the CS plate. Rapid cooling of the A319 sample was obtained as shown in Figure 2 after molten alloy was poured onto the CS plate where it solidified. As shown in Figure 3(a)–(d), the microstructural evolution was clearly observed from the point when the molten alloy first made contact with the impact zone and dendritic microstructures formed to when in the bottom zone of the CS plate nearly spheroidal microstructures of α-Al

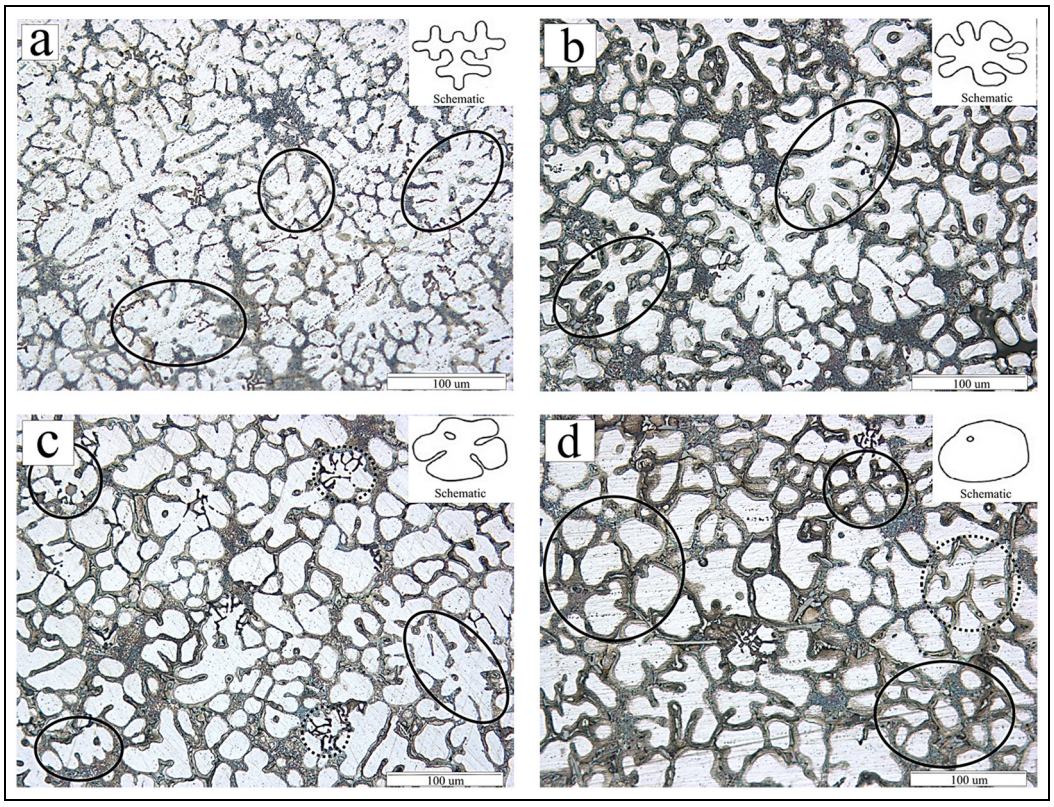

Figure 3. Microstructure of A319 on the CS plate at (a) impact zone, (b) top zone, (c) middle zone and (d) bottom zone, while the inset represents the schematic diagram at the respective zones, that is, dendritic growth stage, rosette, ripened rosette and nearly globular.

were present. The explanation provided by Kirkwood[18] in the form of schematic illustrations is used to explain the evolution of the microstructure obtained in this study as shown in the schematic inset of Figure 3. Four stages of microstructural evolution were apparent. In Figure 3(a), the micrograph is dominated by a dendritic growth structure, but as soon as molten alloy went down CS plate, the dendritic arm structure starts to fragmentize. The beginning of the formation of a nearly spheroidal microstructure was obtained in the bottom zone, as shown in the micrograph in Figure 3(d).

Impact zone of CS plate, Figure 3(a): immediately after the molten alloy makes contact with the plate, it enters the dendritic growth stage. The solid circles on the micrograph highlight examples of this first stage of microstructural evolution in the CS process. In this stage, nucleation of α-Al actively occurs.

Top zone of CS plate, Figure 3(b): the molten alloy enters the rosette growth stage, where the dendritic structures start to evolve into rosette-like shapes. The areas encircled by solid lines highlight examples of these rosettes under formation.

Middle zone of CS plate, Figure 3(c): the alloy enters the ripened rosette stage of its microstructural evolution. In this stage, there are some nearly spheroidal structures in the alloy, but the alloy still primarily consists of ripened rosettes. In this stage, some secondary dendritic arms are broken, as shown by the examples in the dotted circles.

Bottom zone of CS plate, Figure 3(d): the alloy mainly consists of nearly spheroidal microstructures, as shown in the solid circles. However, some ripened rosette microstructures are still present, as highlighted in the dotted circle. Fragmentation of the dendritic arms will occur in the mould by the influence of the cooling rate of the mould.[19]

The phenomenon of microstructural evolution is affected by the shearing process of molten alloy that occurs on the CS plate. The shear force acting between the molten alloy and the CS plate contributes to changing the microstructure of the alloy in the top zone to one that is nearly spheroidal in the bottom zone. Das et al.[20] and Kund and Dutta[21] have investigated the contribution of shearing force to breaking dendritic arms and producing a unique microstructure using the same method as that in this work. A nearly spheroidal microstructure can be referred as equiaxed grains because components within the microstructure having equal dimension are dispersed throughout the alloy. There are three possible mechanisms that can obtain

equiaxed grains, as explained by Kirkwood et al.[22] One is the concept of dendritic arm detachment that explains re-melting process of dendritic arm root on main dendrite through forces created by flow. Bai et al.[23] and Lin et al.[24] used a stirring method to fragmentize the dendritic arms, based on the concept of the shearing force. Another method for achieving a nearly spheroidal microstructure is the SIMA process, which uses recrystallization as the main mechanism instead of the shearing force as applied to CS casting and the stirring method.[25]

The CS plate not only enables contact with a shearing force for fragmentation of α-Al but also acts as a nucleating agent in promoting α-Al. Nucleation is the emergence of a new phase nuclei in first-phase transition.[26] The impact zone of the CS plate has been identified as a hub of nuclei formation because there is a significant temperature difference between the impact zone of the CS plate and the molten alloy. According to Legoretta et al.,[27] the impact zone is the principal source of nuclei. Based on their experiment, they assert that the majority of nucleation occurs in the top part of the CS plate because the microstructure obtained at the end of the CS plate is coarser and the globules size are scattered equally. However, in this work, the microstructures size obtained in the bottom zone (end of the CS plate) were randomly scattered. Thus, the result of this work suggests that there is continuous nucleation during the formation of α-al while the molten alloy flows down the CS plate. That nucleation occurs along the entire CS plate is supported by Taghavi and Ghassemi.[28]

If these two past works by Legoretta et al.[27] and Taghavi and Ghassemi[28] are examined in detail, it becomes apparent that two mechanisms of nucleation are involved in the formation of nuclei in CS casting. Legoretta et al.[27] explain that nucleation occurs in the top part of the CS plate due to the high heat transfer created after the molten alloy has been poured on the top part (impact zone/top zone) of the CS plate. They also conclude that nuclei then coarsen and spheroidize during their descent along the CS plate and state that this is a microstructural development stage and not new nucleation. However, Taghavi and Ghassemi[28] argue that the movement of the melt due to gravity leads to the detachment of the newly formed α-Al phase from the surface or the breaking of the dendritic arms. They conclude that the influence of the CS plate lies in it acting as friction source on the molten alloy. Based on both of these studies, it can be concluded that nucleation occurs homogeneously and heterogeneously, which conforms with kinetic nucleation theory as shown in Figure 4 in general schematic illustration.

Homogeneous nucleation is a process where nuclei arise from the bulk of the liquid itself.[30] During homogeneous nucleation, two energies influence nucleation

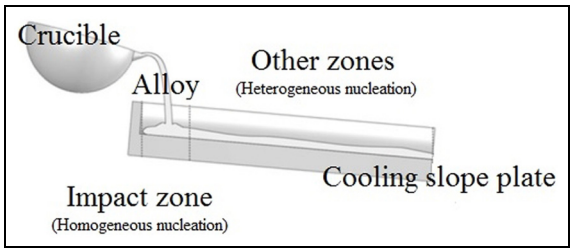

Figure 4. Modified schematic illustration of nucleation mechanism on the cooling slope plate.[29]

formation: (1) the change in bulk free energy as the liquid cools and (2) the surface energy of the nucleating particles.[31] The homogeneous nucleation process occurs when no inoculation is added in the melt. The molten alloy begins to solidify immediately at a temperature below its liquidus point. Elia[31] gives an example of permanent mould casting where nucleating starts at the wall of the mould immediately after molten alloy comes into contact with the cold mould wall. A CS plate with running water underneath assists in promoting a homogeneous nucleation process based on the concept of solidified molten alloy that is applied in permanent mould casting. On the other hand, heterogeneous nucleation occurs when an external nucleating agent such as titanium, boron or strontium has an influence on the mould wall.[32] Fragmentation of the secondary dendritic arm structure on the CS plate will occur due to the shearing force acting on the alloy, indicating the influence of CS plate as mentioned by Teza.[32] According to Taghavi and Ghassemi,[28] solid nuclei are formed because of the contact between the melt and the CS plate, detached from the surface as a result of applied shear stress due to gravitational force and melt flow.

Some factors affect the nucleation process. For instance, Guo et al.[33] and Legoretta et al.[34] explain that the pouring temperature should be close to the liquidus temperature and that the alloy should be quenched quickly to form many nuclei. If the pouring temperature is too high, the molten alloy remains liquid on the CS plate and takes longer to form α-Al. Also, the behaviour of the flow should be taken into consideration when seeking to obtain copious nuclei on the CS plate.[35] The velocity of the flow of molten alloy influences the fragmentation of secondary dendritic arms to produce numerous nuclei. Moreover, an increase in the tilt angle tends to increase the speed at which α-Al breaks up secondary dendritic arms to produce new nucleation.[34]

In summary, nuclei formation either through rapid cooling or shearing force on the CS plate will lead to a nearly spheroidal α-Al microstructure instead of a dendritic microstructure as a result of the CS effect.

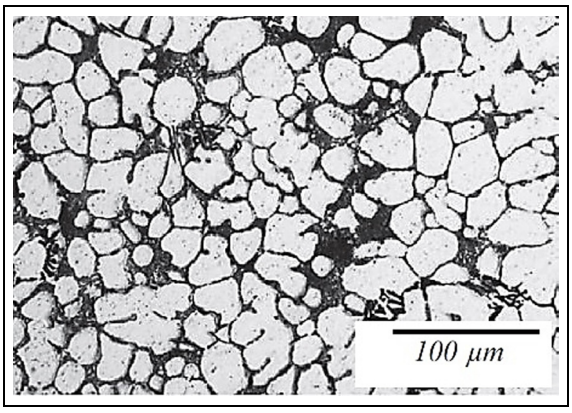

Figure 5. Microstructure of alloy A319 in mould under CS casting process.[6]

Numerous researchers have studied the microstructural changes that occur in the mould after the CS casting process and the mechanical properties of the materials. Curiosity about whether a spheroidal or nearly spheroidal microstructure would be produced on the CS plate led to this work.

This work found that the presence of a mould is necessary in order to obtain a nearly spheroidal microstructure because in the bottom zone the microstructure of the alloy still contains some ripened rosettes, as in dotted circled in micrograph in Figure 3(d). Robert et al.[36] support the theory that the mould and CS plate contribute to the evolution of a nearly spheroidal microstructure. The influence of mould in obtaining a fine globular microstructure is explained in detail by Browne et al.[37] The authors describe the process of rheocasting, which involves pouring an alloy at low superheat into a thin-walled mould. Optimization of the parameters of the CS and mould will enhance the chance of obtaining a nearly globular microstructure or might lead to obtaining a fully globular microstructure. Salleh et al.[6] extended the work of Browne et al.[37] by looking at the microstructure in the mould. If we compare the microstructure produced in the mould in their work (Figure 5) with that in the bottom zone of the CS plate of this work (Figure 3(d)), it can be seen that there is a slight improvement in the globularity of the microstructure.

Mechanism of intermetallic formation in the CS plate

An intermetallic compound is a combination of two or more elements that contribute to the mechanical properties of an alloy. These properties depend on the morphology and chemical formula of the compound. Gencalp Irizalp and Saklakoglu[38] state that the morphology and size of eutectic silicon as well as the morphology and composition of the intermetallic compound have a significant effect on the mechanical properties of alloys. In the case of the aluminium alloy A319, the base elements in the material are aluminium and silicon, but amounts of other elements such as Cu, Mg and Fe are also present. Silicon is a well-known element that has good castability due to its high fluidity and low shrinkage.[39–41] The addition of copper and magnesium can contribute to better strength and corrosion resistance.[42] The formation of the elements will construct a few compounds that commonly exist in A319.

There is a sequence in the phase precipitation of hypoeutectic alloy according to the nucleation phase. Martínez et al.,[43] who used differential thermal analysis (DTA) to investigate the solidification reaction of A319 with added Sr, detected three main peaks of DTA signal that correspond to decreasing temperature: (1) nucleation and growth of α-aluminium, (2) nucleation and growth of Al-Si eutectic and (3) precipitation of multi-phase eutectic such as $\alpha Al + Al_2Cu + Si + Al_5Mg_8Cu_2Si_6$. Another study by Shabestari and Ghodrat[44] explains the main sequence of phase precipitation as follows: (1) formation of α-aluminium, (2) post-dendritic or pre-eutectic phase like $Al_{15}(Fe,Mn)_3Si_2$ (α-phase), (3) main eutectic reaction (Al-Si) and (4) precipitation of post-eutectic phases such as Al_2Cu and Mg_2Si. Five types of intermetallic phases were formed in the A319 alloy by Salleh et al.:[45] Mg_2Si, Al_2Cu, β-Al_5FeSi, π-$Al_9FeMg_3Si_5$ and $Al_5Cu_2Mg_8Si_5$. In this work, intermetallic compounds were detected using SEM to obtain backscatter images of the alloy, as shown in Figure 6 in which the following are highlighted: $Al_{15}(Fe,Mn)_3Si_2$ (arrow 1), Al_5FeSi (arrow 2), Al_2Cu (arrow 3), eutectic Si (arrow 4) and Mg_2Si (arrow 5).

Among all these compounds, the iron-rich metallic compound is the most undesired because it causes brittleness. Both Narayanan et al.[46] and Salleh et al.[45] agree that the effect of iron in aluminium alloys can lead to reduced tensile strength and ductility. Two phases of iron were found in this work, namely α-phase and β-phase, as indicated by arrows 1 and 2 in Figure 6, respectively. Both of these phases were found along the entirety of the CS plate. $Al_{15}(Fe,Mn)_3Si_2$ and Al_5FeSi are the two iron metallic compounds that indicate the stoichiometry of the α-phase and β-phase, respectively.[44] In the sample, the intermetallic compound of the α-phase had a Chinese script morphology and it looks grey; however, it can also appear as a polyhedral morphology. Low or high iron and manganese content contributes to the Chinese script and polyhedral morphology, respectively.[47] In this work, no polyhedral morphology was detected in the alloy for any zone of the CS plate, indicating that this alloy contained low iron and manganese. The β-phase is another form of α-phase in the form of a needle-like iron intermetallic

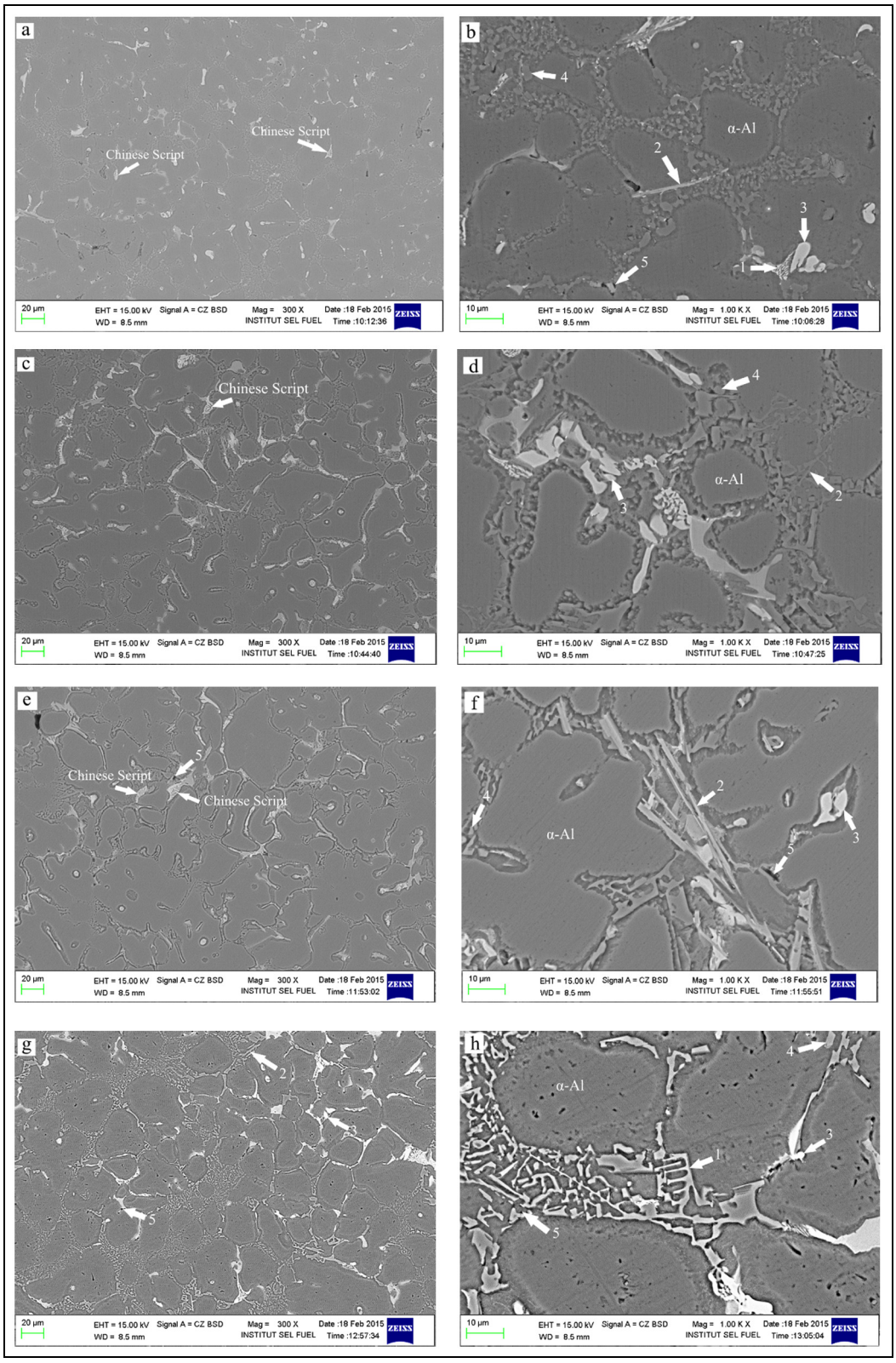

Figure 6. SEM backscatter images of A319 alloy in (a and b) impact zone, (c and d) top zone, (e and f) middle zone and (g and h) bottom zone.
Arrow 1: $Al_{15}(Fe,Mn)_3Si_2$; arrow 2: Al_5FeSi; arrow 3: Al_2Cu; arrow 4: eutectic Si; arrow 5: Mg_2Si.

compound and was identified in the alloy on the CS plate (see Figure 6). The existence of the β-phase in the alloy has a more harmful effect on its mechanical properties than the α-phase. Converting the β-phase morphology to an α-phase morphology minimizes the detrimental effect of iron. According to Narayanan et al.,[46] there are three basic methods that can be used to convert the β-phase to the α-phase: (1) rapid solidification, (2) manganese addition and (3) melt superheating. The most common method to neutralize the iron effect is making sure there is a proper ratio of iron to manganese.

Figure 6 shows that Al_2Cu has a compact and blocky shape, as indicated by arrow 3. According to Shabestari and Ghodrat,[44] the formation of the Al_2Cu phase occurs at 503°C during alloy solidification. The brittle behaviour of alloy can be related to the formation of the intermetallic compound Al_2Cu.[48] Another phase that was found in the sample was Mg_2Si. Arrow 5 in Figure 6 points to the presence of black fine particles of the Mg_2Si compound in the alloy from certain zones of the CS plate. The Mg_2Si compound provides strength and hardening in the form of a fine dispersion of particles in the alloy.[49] According to Qin et al.,[50] an intermetallic compound of Mg_2Si contributes good mechanical properties to alloy by providing high hardness, reasonably high elastic modulus and low thermal expansion. The size of Mg_2Si is detected fine in this work as contribution of CS plate mechanism and it was supported by Qin et al.[50] The flow of the melt on the CS plate is one of the factors that influences the fineness of the compound.

The elements of alloying have an influence on an alloy's mechanical properties and microstructure. As discussed earlier, some intermetallic compounds such as iron-rich intermetallic compounds can have an adverse effect on a material's mechanical properties. However, elements of alloying such as Mg_2Si can have a positive influence by assisting in achieving a refinement in the size and sphericity of α-Al particles. According to Nafisi and Ghomashchi,[51] dissolved titanium on primary α-Al has an effect on grain size in the semi-solid casting of A356 alloy. They found that solute Ti could restrict the size of globule grain in the semi-solid casting process by explaining grain growth restriction mechanism as an argument to grain refinement mechanism process that explain on more effective nucleation, not the restriction capability of Ti. In another study, Phongphisutthinan et al.[52] investigated how to control the semi-solid microstructure of wrought Al-Mg-Si alloys with Fe and Mn in the deformation-semi-solid-forming process. The authors stated that the fragmentation of the Fe-intermetallic compound and the AlFeMnSi compound is useful in refining α-Al grains when using this process.

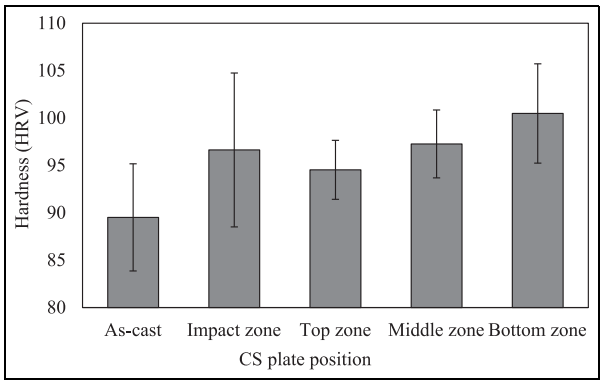

Figure 7. Comparison of as-cast hardness with hardness of A319 in four different positions on the CS plate.

Mechanical properties

The hardness of A319 as-cast and in all four zones in this work is shown in Figure 7. The hardness of the as-cast sample of A319 was 89.51 ± 5.6 HV, whereas the hardness of A319 in the bottom zone of the CS plate was 100.47 ± 5.2 HV. The percentage increment in hardness was 12.2% by the CS casting process as compared to the as-cast A319. A comparison of hardness for all four zones on the CS plate showed a minor difference; however, there was still an increment between the impact zone and the bottom zone. The Vickers reading obtained in this study was in the range of hardness obtained by Salleh et al.[6] of approximately 89.7 ± 4.4 HV for the as-cast sample and 104 ± 2.7 HV for the thixoforming sample. The hardness of the material increased due to the microstructure of α-Al becoming progressively more spheroidal compared to the as-cast sample. According to Burapa et al.,[53] mechanical properties are affected by the shape factor and grain size of the primary α-Al. They further explain that the relationship between the mechanical properties and the shape factor of primary phase α-Al is directly proportional. As seen in Figure 7, the alloy exhibited slightly less hardness in the top zone compared to that in the impact zone. If the globularity of α-Al is taken into account, this situation should not occur due to the mechanism of evolution, as previously discussed. In Figure 6(d), the intermetallic compound of Mg_2Si was not detected and thus was not available to strengthen the alloy. This contributed to the lower amount of hardness in the alloy in the top zone of the CS plate.

Conclusion

The study has successfully captured the microstructure developments at four different zones along the CS plate. These microstructures support the schematic diagrams representing the stages discussed in various

previous works. A globular microstructure would be obtained through the shearing force on the CS plate plus the influence of a cooling rate in the mould. This study also showed that homogeneous and heterogeneous nucleations influenced the globularization of the solid nuclei. Moreover, this study also identified some intermetallic compounds such as Al_5FeSi, Mg_2Si, Al_2Cu and $Al_{15}(Fe,Mn)_3Si_2$ on the CS plate. The formation of the Mg_2Si compound was particularly important as its fine dispersion assists in the refinement and sphericity of the α-Al particles, as well as providing strength and hardness to the alloy.

Declaration of conflicting interests

The author(s) declared no potential conflicts of interest with respect to the research, authorship and/or publication of this article.

Funding

The author(s) disclosed receipt of the following financial support for the research, authorship and/or publication of this article: The authors would like to thank Universiti Kebangsaan Malaysia (UKM; The National University of Malaysia) and Ministry of Higher Education Malaysia for the financial support received under research grants DIP-2014-024 and FRGS/1/2014/TK01/UKM/01/2.

References

1. Koeune R. *Semi-solid constitutive modeling for the numerical simulation of thixoforming processes*. PhD Thesis, Universitè de Liège, Liège, 2011.
2. Ahmad AH, Naher S, Aqida S, et al. Routes to spheroidal starting material for semisolid metal processing. *Compr Mater Process* 2014; 5: 135–148.
3. Haga T and Suzuki S. Casting of aluminum alloy ingots for thixoforming using a cooling slope. *J Mater Process Tech* 2001; 118: 169–172.
4. Haga T and Kapranos P. Simple rheocasting processes. *J Mater Process Tech* 2002; 130–131: 594–598.
5. Haga T and Kapranos P. Billetless simple thixoforming process. *J Mater Process Tech* 2002; 130–131: 581–586.
6. Salleh MS, Omar MZ, Syarif J, et al. Microstructure and mechanical properties of thixoformed A319 aluminium alloy. *Mater Design* 2014; 64: 142–152.
7. Rosso M. Thixocasting and rheocasting technologies, improvements going on. *J Achiev Mater Manuf Eng* 2012; 54: 110–119.
8. Zeren M. Effect of copper and silicon content on mechanical properties in Al–Cu–Si–Mg alloys. *J Mater Process Tech* 2005; 169: 292–298.
9. Ejiofor JU and Reddy RG. Developments in the processing and properties of particulate Al-Si composites. *JOM* 1997; 49: 31–37.
10. Lu S and Hellawell A. Modification of Al-Si alloys: microstructure, thermal analysis, and mechanisms. *JOM* 1995; 47: 38–40.
11. Hrivnak N. *ASM specialty handbook: aluminum and aluminum alloys*. Materials Park, OH: ASM International, 1996, p.784.
12. Gruzleski JE and Closset BM. *The treatment of liquid aluminum-silicon alloys*. Des Plaines, IL: American Foundrymen's Society, Incorporated, 1990, p.256.
13. Legoretta EC, Atkinson HV and Jones H. Cooling slope casting to obtain thixotropic feedstock. In: *Proceedings of the 5th decennial international conference on solidification processing*, Sheffield, 23–25 July 2007, pp.582–586. Southampton: White Rose Research Online.
14. Das P, Samanta SK, Venkatpathi BRK, et al. Microstructural evolution of A356 Al alloy during flow along a cooling slope. *T Indian I Metals* 2012; 65: 669–672.
15. Liu D, Atkinson HV and Jones H. Thermodynamic prediction of thixoformability in alloys based on the Al–Si–Cu and Al–Si–Cu–Mg systems. *Acta Mater* 2005; 53: 3807–3819.
16. Arif MAM, Omar MZ, Muhamad N, et al. Microstructural evolution of solid-solution-treated Zn–22Al in the semisolid state. *J Mater Sci Technol* 2013; 29: 765–774.
17. Birol Y. Thixoforming of non-dendritic AA6061 feedstock produced by low superheat casting with and without a cooling slope. *Int J Mater Res* 2007; 98: 1019–1024.
18. Kirkwood DH. Semisolid metal processing. *Int Mater Rev* 1994; 39: 173–189.
19. Legoretta EC, Atkinson HV and Jones H. Microstructural evolution of A356 during NRC processing. In: *Proceedings of the 8th international conference on semi-solid processing of alloys and composites (S2P '04)*, Limassol, 21–23 September 2004, pp.673–684. Warrendale, PA: TMS.
20. Das P, Samanta SK, Ray T, et al. Mechanical properties and tensile fracture mechanism of rheocast A356 Al alloy using cooling slope. *Adv Mat Res* 2012; 585: 354–358.
21. Kund NK and Dutta P. Numerical simulation of solidification of liquid aluminum alloy flowing on cooling slope. *T Nonferr Metal Soc* 2010; 20: 898–905.
22. Kirkwood DH, Suéry M, Kapranos P, et al. *Semi-solid processing of alloys*. New York; Berlin; Heidelberg: Springer, 2010, p.170.
23. Bai F, Sha M, Li T, et al. Influence of rotating magnetic field on the microstructure and phase content of Ni–Al alloy. *J Alloy Compd* 2011; 509: 4835–4838.
24. Lin X, Tong L, Zhao L, et al. Morphological evolution of non-dendritic microstructure during solidification under stirring. *T Nonferr Metal Soc* 2010; 20: 826–831.
25. Bolouri A, Shahmiri M and Cheshmeh ENH. Microstructural evolution during semisolid state strain induced melt activation process of aluminum 7075 alloy. *T Nonferr Metal Soc* 2010; 20: 1663–1671.
26. Ruckenstein E, Berim GO and Narsimhan G. A novel approach to the theory of homogeneous and heterogeneous nucleation. *Adv Colloid Interfac* 2015; 215: 13–27.
27. Legoretta EC, Atkinson HV and Jones H. Cooling slope casting to obtain thixotropic feedstock II: observations with A356 alloy. *J Mater Sci* 2008; 43: 5456–5469.
28. Taghavi F and Ghassemi A. Study on the effects of the length and angle of inclined plate on the thixotropic microstructure of A356 aluminum alloy. *Mater Design* 2009; 30: 1762–1767.

29. Bünck M, Warnken N and Bührig-Polaczek A. Microstructure evolution of rheo-cast A356 aluminium alloy in consideration of different cooling conditions by means of the cooling channel process. *J Mater Process Tech* 2010; 210: 624–630.
30. Gruzleski JE. *Microstructure development during metal-casting*. Des Plaines, IL: American Foundrymen's Society, Incorporated, 2000, p.244.
31. Elia FD. *A study on grain refinement and hot tearing in permanent mold cast aluminum alloys*. MSc Thesis, Ryerson University, Toronto, ON, Canada, 2009.
32. Teza H. *Grain refinement and nucleation processes in aluminium alloys through liquid shearing*. PhD Thesis, Brunel University London, Uxbridge, 2009.
33. Guo HM, Yang XJ and Hu B. Rheocasting of A356 alloy by low superheat pouring with a shearing field. *Acta Metall Sin* 2006; 19: 328–334.
34. Legoretta EC, Atkinson HV and Jones H. Cooling slope casting to obtain thixotropic feedstock I: observations with a transparent analogue. *J Mater Sci* 2008; 43: 5448–5455.
35. Xiao-li Z, Ting-ju L, Shui-sheng X, et al. Microstructure evolution of A356 alloy in a novel rheocasting approach. *J Mater Process Tech* 2009; 209: 2092–2098.
36. Robert MH, Zoqui EJ, Tanabe F, et al. Producing thixotropic semi-solid A356 alloy: microstructure formation x forming behaviour. *J Achiev Mater Manuf Eng* 2007; 20: 19–26.
37. Browne DJ, Hussey MJ, Carr AJ, et al. Direct thermal method: new process for development of globular alloy microstructure. *Int J Cast Metal Res* 2003; 16: 418–426.
38. Gencalp Irizalp S and Saklakoglu N. Effect of Fe-rich intermetallics on the microstructure and mechanical properties of thixoformed A380 aluminum alloy. *Eng Sci Technol* 2014; 17: 58–62.
39. Javidani M and Larouche D. Application of cast Al–Si alloys in internal combustion engine components. *Int Mater Rev* 2014; 59: 132–158.
40. Solek KP, Kuziak RM and Karbowniczek M. The application of thermodynamic calculations for the semi-solid processing design. In: *Proceedings of the symposium I 'phase diagrams; phase stability; theory and applications'*, Warsaw, 4–8 September 2006, pp.4–8. Kraków: Archives of Metallurgy and Materials.
41. Hegde S and Prabhu KN. Modification of eutectic silicon in Al–Si alloys. *J Mater Sci* 2008; 43: 3009–3027.
42. Rana RS, Purohit R and Das S. Reviews on the influences of alloying elements on the microstructure and mechanical properties of aluminum alloys and aluminum alloy composites. *Int J Sci Res Publ* 2012; 2: 1–7.
43. Martínez EJD, Cisneros GMA, Valtierra S, et al. Effect of strontium and cooling rate upon eutectic temperatures of A319 aluminum alloy. *Scripta Mater* 2005; 52: 439–443.
44. Shabestari SG and Ghodrat S. Assessment of modification and formation of intermetallic compounds in aluminum alloy using thermal analysis. *Mat Sci Eng A: Struct* 2007; 467: 150–158.
45. Salleh MS, Omar MZ and Syarif J. The effects of Mg addition on the microstructure and mechanical properties of thixoformed Al–5%Si–Cu alloys. *J Alloy Compd* 2015; 621: 121–130.
46. Narayanan LA, Samuel FH and Gruzleski JE. Crystallization behavior of iron-containing intermetallic compounds in 319 aluminum alloy. *Metall Mater Trans A* 1994; 25: 1761–1773.
47. Shabestari SG and Parshizfard E. Effect of semi-solid forming on the microstructure and mechanical properties of the iron containing Al–Si alloys. *J Alloy Compd* 2011; 509: 7973–7978.
48. Rincon E, Lopez HF, Cisneros MM, et al. Temperature effects on the tensile properties of cast and heat treated aluminum alloy A319. *Mat Sci Eng A: Struct* 2009; 519: 128–140.
49. Velasco E, Col R, Valtierra S, et al. A model for thermal fatigue in an aluminium casting alloy. *Int J Fatigue* 1995; 17: 399–406.
50. Qin QD, Zhao YG, Cong PJ, et al. Semisolid microstructure of Mg_2Si/Al composite by cooling slope cast and its evolution during partial remelting process. *Mat Sci Eng A: Struct* 2007; 444: 99–103.
51. Nafisi S and Ghomashchi R. The effect of dissolved titanium on the primary α-Al grain and globule size in the conventional and semi-solid casting of 356 Al–Si Alloy. *J Mater Sci* 2006; 41: 7954–7963.
52. Phongphisutthinan C, Tezuka H and Sato T. Semi-solid microstructure control of wrought Al-Mg-Si based alloys with Fe and Mn additions in deformation-semi-solid-forming process. *Mater T JIM* 2011; 52: 834–841.
53. Burapa R, Janudom S, Chucheep T, et al. Effects of primary phase morphology on mechanical properties of Al-Si-Mg-Fe alloy in semi-solid slurry casting process. *T Nonferr Metal Soc* 2010; 20: 857–861.